

# First-principles study on the stability of $(R, \text{Zr})(\text{Fe}, \text{Co}, \text{Ti})_{12}$ against 2-17 and unary phases ( $R = \text{Y}, \text{Nd}, \text{Sm}$ )

Taro Fukazawa,<sup>1,2,\*</sup> Yosuke Harashima,<sup>1,2,3,4</sup> and Takashi Miyake<sup>1,2</sup>

<sup>1</sup>*CD-FMat, National Institute of Advanced Industrial Science and Technology, Tsukuba, Ibaraki 305-8568, Japan*

<sup>2</sup>*ESICMM, National Institute for Materials Science, Tsukuba, Ibaraki 305-0047, Japan*

<sup>3</sup>*Center for Computational Sciences, University of Tsukuba, Tsukuba, Ibaraki 305-8577, Japan*

<sup>4</sup>*Division of Materials Science, Nara Institute of Science and Technology, Ikoma, Nara 630-0192, Japan*

(Dated: March 29, 2022)

The stability of  $(R, \text{Zr})(\text{Fe}, \text{Co}, \text{Ti})_{12}$  with a  $\text{ThMn}_{12}$  structure is investigated using first-principles calculations. We consider energetic competition with multiple phases that have the  $\text{Th}_2\text{Zn}_{17}$  structure and the unary phases of  $R$ ,  $\text{Zr}$ ,  $\text{Fe}$ ,  $\text{Co}$ , and  $\text{Ti}$  simultaneously by constructing a quinary energy convex hull. From the analysis, we list the stable phases at zero temperature, and show possible stable and metastable  $\text{ThMn}_{12}$  phases.

PACS numbers: TBD

Keywords: TBD

## I. INTRODUCTION

Magnet compounds with the  $\text{ThMn}_{12}$  structure have attracted attention as possible main phases for high-performance magnets [1–19]. Hirayama et al. recently reported that films of  $\text{NdFe}_{12}\text{N}$ ,  $\text{SmFe}_{12}$ , and  $\text{Sm}(\text{Fe}, \text{Co})_{12}$  have magnetic properties superior to those of  $\text{Nd}_2\text{Fe}_{14}\text{B}$ , which is the main phase of the current best magnet.  $R\text{Fe}_{12}$  ( $R$  = rare earth) compounds with the  $\text{ThMn}_{12}$  structure achieve high magnetization owing to the large Fe content. However, the thermodynamic instability of these compounds is an obstacle for developing practical magnets.

Introducing a third element can stabilize the structure of these compounds in the bulk material [5, 8, 20]. Ti is a typical stabilizing element, although it occupies the Fe sites in  $R\text{Fe}_{12}$ , and thus the magnetization is reduced due to the decrease in the Fe content. Moreover, the magnetic moment of Ti couples antiferromagnetically to the host. In the search for an efficient stabilizer, several transition elements have been found to behave similarly to Ti.  $R$ -site doping is another approach to stabilization, and Zr is a potential stabilizer because it mainly dopes the  $R$  site and simultaneous doping with Zr and Ti may reduce the amount of Ti required for stabilization [21–24]. When the Ti content is small, the system tends to form structures related to the  $\text{Th}_2\text{Zn}_{17}$ - or  $\text{Th}_2\text{Ni}_{17}$ -structure (the 2-17 phase). Y is another possible  $R$ -site doping stabilizer.  $\text{YFe}_{12}$  is also obtained by the rapid quenching method, and coexists with a 2-17 related phase that has the  $\text{TbCu}_7$  structure [25].  $\text{YFe}_{12}$  decomposes into the 2-17 phase and  $\alpha$ -Fe at a higher temperatures.

Several theoretical studies have searched for efficient stabilizing elements. We have investigated the stability and magnetism in  $\text{NdFe}_{11}M$  for  $M = \text{Ti}, \text{V}, \text{Cr}, \text{Mn}, \text{Fe}, \text{Co}, \text{Ni}, \text{Cu}, \text{Zn}$  by using first-principles calculations,

and we suggested that Co could function as a stabilizing third element [26]. The effect of the  $R$ -site substitution in  $R\text{Fe}_{12}$  was also studied for  $R = \text{La}, \text{Pr}, \text{Sm}, \text{Gd}, \text{Dy}, \text{Ho}, \text{Er}, \text{Tm}, \text{Lu}, \text{Y}, \text{Sc}, \text{Zr}, \text{Hf}$  [27]. In the paper, we considered the stability against the  $R_2\text{Fe}_{17}$  phases and suggested some rare-earth elements, including Y, as possible stabilizers. However, how the proposed elements work as a dopant, when the amount is fractional per unit cell, remains theoretically unexplored. The effects of co-doping have not been theoretically investigated for those systems either.

In this paper, we consider the stability of  $(R, \text{Zr})(\text{Fe}, \text{Co}, \text{Ti})_{12}$  to reveal how the dopant stabilizes the  $\text{ThMn}_{12}$  structure. We consider the unary phases ( $R, \text{Zr}, \text{Fe}, \text{Co}, \text{Ti}$ ) and the  $R_2(\text{Fe}, \text{Co})_{17}$  phases with the  $\text{Th}_2\text{Zn}_{17}$  structure as competing phases simultaneously. In treating the randomness caused by the doping, we use coherent potential approximation (CPA). We also use a previously proposed method to improve the data from the CPA with a small number of accurate data from a different origin [28]. We generate a quinary phase diagram by constructing an energy convex hull, and predict the stable phases at zero temperature within the scope of the calculation. We also discuss the stability of the  $(R, \text{Zr})(\text{Fe}, \text{Co}, \text{Ti})_{12}$  phases based on their energy differences (hull distance) from the boundary of the convex hull and compare the values with previous experimental reports.

## II. METHODOLOGY

We perform first-principles calculations based on density functional theory within the local density approximation [29, 30]. In solving the Kohn-Sham problem, we use AkaiKKR (MACHIKANEYAMA) [31], which is based on the Korringa-Kohn-Rostoker Green function method [32, 33]. For the f-electrons in Nd and Sm, the open-core approximation [34–36] is used, and the self-interaction correction is applied [37]. Calculations of

\* E-mail: taro.fukazawa@aist.go.jp

$(R_{1-\alpha}Zr_\alpha)(Fe_{1-\beta}Co_\beta)_{12-\gamma}Ti_\gamma$  with the  $ThMn_{12}$  structure,  $R_2(Fe_{1-\beta}Co_\beta)_{17}$ , and  $Zr_2(Fe_{1-\beta}Co_\beta)_{17}$  with the  $Th_2Zn_{17}$  structure are performed for  $\alpha$  from 0 to 1 with an interval of 0.1,  $\beta$  from 0 to 1 with an interval of 0.1, and  $\gamma$  from 0 to 1 with an interval of 0.5 ( $R = Y, Nd, Sm$ ). The lattice parameters are obtained by linearly interpolating parameters from referential data. These reference values are obtained by first-principles calculations for  $RFe_{12}$ ,  $ZrFe_{12}$ ,  $RFe_{11}Ti$ ,  $ZrFe_{11}Ti$ ,  $RCO_{12}$ ,  $R_2Fe_{17}$ ,  $Zr_2Fe_{17}$ ,  $R_2Co_{17}$ , and  $Zr_2Co_{17}$  using QMAS, [38] which is based on the projector-augmented-wave method [39, 40].

In treating the randomness caused by the doping, we use coherent potential approximation (CPA), where electronic backscattering from the randomized environment is approximated by an effective medium which is self-consistently determined in terms of the configuration average of the Green function.[41–43] However, calculating energy with the CPA tends to need much computational resources when high accuracy is needed owing to the use of localized bases in the CPA. To overcome this problem, we use a recently proposed method for improving a data set with another data set from a different origin by constructing a stochastic model [28]. In the current case, we apply this to the large data obtained with the CPA and a small amount of reference data, which are also used in the interpolation for lattice parameters above.

To investigate the stability, we construct an energy convex hull. It is convenient to introduce coordinates  $\eta = (\zeta_1, \zeta_2, \zeta_3, \zeta_4, \varepsilon)$  for a quinary system  $R_{1-\zeta_1-\zeta_2-\zeta_3-\zeta_4}Zr_{\zeta_1}Fe_{\zeta_2}Co_{\zeta_3}Ti_{\zeta_4}$ , where  $\varepsilon$  denotes the total energy per formula. When there are two systems, which are  $\eta^{(1)}$  and  $\eta^{(2)}$  in this coordinate space, the composition and energy of separate phases of  $\eta^{(1)}$  and  $\eta^{(2)}$  can be described as a linear interpolation of these two points. This concept can extend to phase separation into five different phases, which corresponds to a five-dimensional facet that has five vertices, where a vertex represents a single phase. In principle, the stable phases can be obtained by constructing facets from all the combinations of the vertices and finding the energetically lowest facets. The vertices of the lowest facets represent the stable phases.

We perform this part of the data analysis by using qhull, a package for efficiently constructing a convex hull from given data points [44, 45]. This program also generates the upper part of a convex hull, which is unnecessary for our purpose, although it is easy to remove by checking the direction of the normal vector for each facet.

### III. RESULTS AND DISCUSSION

#### A. Stable phases

Tables I, II, and III show the stable phases obtained by the hull construction for  $R = Y, Nd, Sm$ , respectively. Ti-lean systems are of interest because Ti-doping of  $(R,Zr)(Fe,Co)_{12}$  reduces the magnetization of a system

TABLE I. Stable phases in the Y–Zr–Fe–Co–Ti system. The calculated values of the magnetization are 1.76 T for  $(Y_{0.1}Zr_{0.9})Fe_{12}$ , and 1.74 T for  $Zr(Fe_{0.9}Co_{0.1})_{12}$ .

Unary Y, Zr, Fe, Co, Ti
$(Y_{0.1}Zr_{0.9})Fe_{12}$
$Zr(Fe_{0.9}Co_{0.1})_{12}$
$(Y_{1-\alpha}Zr_\alpha)Fe_{11}Ti$ ( $\alpha = 0, 0.1, 0.2, 1$ )
$(Y_{1-\alpha}Zr_\alpha)Co_{11}Ti$ ( $\alpha = 0, 0.1, 0.2, 0.7, 0.8, 0.9, 1$ )
$Y(Fe_{1-\beta}Co_\beta)_{11}Ti$ ( $\beta = 0-1$ )
$Y_2(Fe_{1-\beta}Co_\beta)_{17}$ ( $\beta = 0, 0.4, 0.5, 0.6, 0.7, 0.8, 0.9, 1$ )
$Zr_2(Fe_{1-\beta}Co_\beta)_{17}$ ( $\beta = 0, 0.5, 0.6, 0.7, 0.8, 0.9, 1$ )

TABLE II. Stable phases in the Nd–Zr–Fe–Co–Ti system. The calculated values of the magnetization are 1.76 T for  $Nd_{0.1}Zr_{0.9}Fe_{12}$  and 1.74 T, 1.69 T, 1.64 T, 1.60 T, 1.54 T for  $Zr(Fe_{1-\beta}Co_\beta)_{12}$  ( $\beta = 0.1, 0.2, 0.3, 0.4, 0.5$ ), respectively.

Unary Nd, Zr, Fe, Co, Ti
$Nd_{0.1}Zr_{0.9}Fe_{12}$
$Zr(Fe_{1-\beta}Co_\beta)_{12}$ ( $\beta = 0.1, 0.2, 0.3, 0.4, 0.5$ )
$Nd(Fe_{1-\beta}Co_\beta)_{11}Ti$ ( $\beta = 0-1$ )
$(Nd_{0.9}Zr_{0.1})Fe_{11}Ti$
$ZrFe_{11}Ti$
$(Nd_{1-\alpha}Zr_\alpha)Co_{11}Ti$ ( $\alpha = 0.5, 0.6, 0.8, 0.9, 1$ )
$Nd_2(Fe_{1-\alpha}Co_\alpha)_{17}$ ( $\alpha = 0.5, 0.6, 0.8, 0.9, 1$ )
$Zr_2(Fe_{1-\alpha}Co_\alpha)_{17}$ ( $\alpha = 0, 0.9, 1$ )

by substituting Fe and Co. The Zr-rich systems without Ti are predicted to be stable. There are differences in the range of Co content for  $Zr(Fe,Co)_{12}$  due to the differences in the lattice constants used in the calculations, which are deduced by linear interpolation for each of the  $R = Y, Nd, Sm$  cases. However, the general trends are similar and the systems tend to be stable with a high Zr content and low Co content. The estimated magnetizations of the stable Ti-less  $ThMn_{12}$  phases (shown in the captions of the tables) are higher than the estimated value of 1.49 T for  $Nd_2Fe_{14}B$ . [46]

Figures 1, 2, and 3 show the phase diagrams for the  $R = Y, Nd, Sm$  cases, respectively. These are obtained by projecting the lowest facets of the convex hull to the  $(R,Zr)(Fe,Co)_{12}$  plane, that is, the plane of  $\zeta_2 + \zeta_3 + \zeta_4 = 12/13$ , which constrains the ratio of  $Fe + Co + Ti$  to  $R + Zr$ ,  $\zeta_4 = 0$  (no Ti), and  $\varepsilon = \text{const}$ . Therefore, these diagrams show how the 1-12 compositions separate into stable phases at zero temperature.

The  $ThMn_{12}$  phases are found only in a limited region of the diagrams, whereas the 2-17 phase appears everywhere in the planes, except for the edges of regions, demonstrating how the 2-17 phase is important in considering the stability of the  $ThMn_{12}$  structure.

Related to the stabilization effect of Zr, Friedel and Sayers discussed the role of d–d correlations in cohesion, and discussed that the cohesive energy tends to

TABLE III. Stable phases in the Sm-Zr-Fe-Co-Ti system. The calculated values of the magnetization are 1.76 T for  $(\text{Sm}_{0.1}\text{Zr}_{0.9})\text{Fe}_{12}$  and 1.74 T, 1.69 T, 1.64 T for  $\text{Zr}(\text{Fe}_{1-\beta}\text{Co}_{\beta})_{12}$  ( $\beta = 0.1, 0.2, 0.3$ ) respectively.

Unary Sm, Zr, Fe, Co, Ti
$(\text{Sm}_{0.1}\text{Zr}_{0.9})\text{Fe}_{12}$
$\text{Zr}(\text{Fe}_{1-\beta}\text{Co}_{\beta})_{12}$ ( $\beta = 0.1, 0.2, 0.3$ )
$\text{Sm}(\text{Fe}_{1-\beta}\text{Co}_{\beta})\text{Ti}$ ( $\beta = 0-1$ )
$(\text{Sm}_{0.9}\text{Zr}_{0.1})\text{Fe}_{11}\text{Ti}$
$\text{ZrFe}_{11}\text{Ti}$
$\text{ZrCo}_{11}\text{Ti}$
$\text{Sm}_2(\text{Fe}_{1-\alpha}\text{Co}_{\alpha})_{17}$ ( $\alpha = 0.5, 0.6, 0.7, 0.9, 1$ )
$\text{Zr}_2(\text{Fe}_{1-\alpha}\text{Co}_{\alpha})_{17}$ ( $\alpha = 0, 0.7, 0.8, 0.9, 1$ )

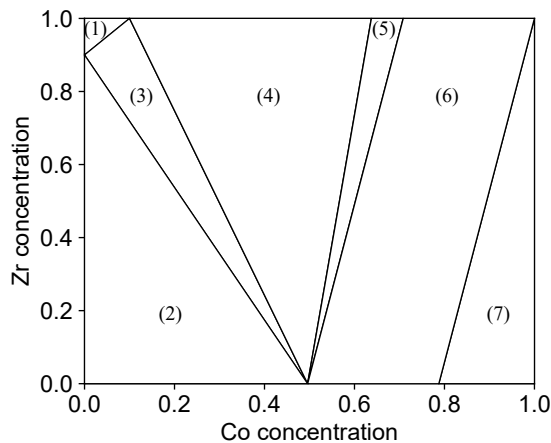


FIG. 1. Phase diagram on the  $(\text{Y,Zr})(\text{Fe,Co})_{12}$  plane. (1)  $(\text{Y,Zr})\text{Fe}_{12}$ ,  $\text{Zr}(\text{Fe,Co})_{12}$ ,  $\text{Zr}_2\text{Fe}_{17}$ , and unary Fe; (2)  $(\text{Y,Zr})\text{Fe}_{12}$ ,  $\text{Y}_2(\text{Fe,Co})_{17}$ , and unary Fe; (3)  $(\text{Y,Zr})\text{Fe}_{12}$ ,  $\text{Zr}(\text{Fe,Co})_{12}$ ,  $\text{Y}_2(\text{Fe,Co})_{17}$ , and unary Fe; (4)  $\text{Zr}(\text{Fe,Co})_{12}$ ,  $\text{Y}_2(\text{Fe,Co})_{17}$ ,  $\text{Zr}_2(\text{Fe,Co})_{17}$ , and unary Fe; (5)  $\text{Y}_2(\text{Fe,Co})_{17}$ ,  $\text{Zr}_2(\text{Fe,Co})_{17}$ , and unary Fe; (6)  $\text{Y}_2(\text{Fe,Co})_{17}$ ,  $\text{Zr}_2\text{Co}_{17}$ , and unary Fe and Co; (7)  $\text{Y}_2(\text{Fe,Co})_{17}$ ,  $\text{Zr}_2\text{Co}_{17}$ , and unary Co.

increase when the number of electrons changes toward half-filling.[47] They also suggested that broadening of the band width is preferable for cohesion, which is discernible in comparison between the Y system and Zr system in Fig. 4.

The stabilization of the  $\text{ThMn}_{12}$  phase against the  $\text{Th}_2\text{Zn}_{17}$  phase by introducing Zr may be explained by the difference in DOS. In  $\text{ZrFe}_{12}$ , the Fermi level is placed in a sharper dip in the minority band than in  $\text{Zr}_2\text{Fe}_{17}$ , and DOS at the Fermi level is close to that in  $\text{Zr}_2\text{Fe}_{17}$ . In terms of the band energy, the DOS of  $\text{ZrFe}_{12}$  is more preferable under addition and removal of a small amount of electrons, which corresponds to addition of Co and R).

No system with  $\gamma = 0.5$  is stable in this search for  $(\text{R}_{1-\alpha}\text{Zr}_{\alpha})(\text{Fe}_{1-\beta}\text{Co}_{\beta})_{12-\gamma}\text{Ti}_{\gamma}$  stable phases. Ti may be distributed inhomogeneously in separate phases of the

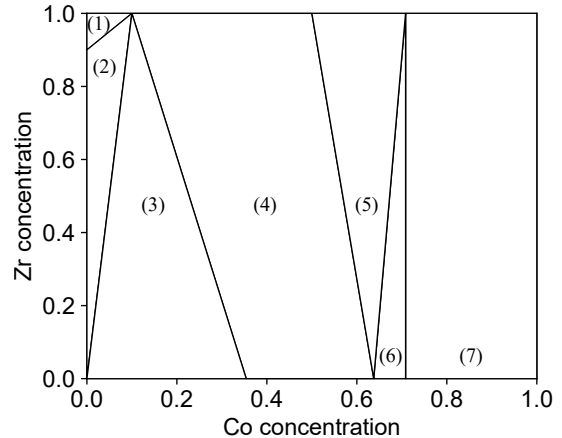


FIG. 2. Phase diagram on the  $(\text{Nd,Zr})(\text{Fe,Co})_{12}$  plane. (1)  $(\text{Nd,Zr})\text{Fe}_{12}$ ,  $\text{Zr}(\text{Fe,Co})_{12}$ ,  $\text{Zr}_2\text{Fe}_{17}$ , and unary Fe; (2)  $(\text{Nd,Zr})\text{Fe}_{12}$ ,  $\text{Zr}(\text{Fe,Co})_{12}$ , and unary Nd and Fe; (3)  $\text{Zr}(\text{Fe,Co})_{12}$ ,  $\text{Nd}_2(\text{Fe,Co})_{17}$ , and unary Nd and Fe; (4)  $\text{Zr}(\text{Fe,Co})_{12}$ ,  $\text{Nd}_2(\text{Fe,Co})_{17}$ , and unary Fe; (5)  $\text{Zr}(\text{Fe,Co})_{12}$ ,  $\text{Nd}_2(\text{Fe,Co})_{17}$ ,  $\text{Zr}_2\text{Co}_{17}$ , and unary Fe; (6)  $\text{Nd}_2(\text{Fe,Co})_{17}$ ,  $\text{Zr}_2\text{Co}_{17}$ , and unary Fe; (7)  $\text{Nd}_2(\text{Fe,Co})_{17}$ ,  $\text{Zr}_2\text{Co}_{17}$ , and unary Fe and Co.

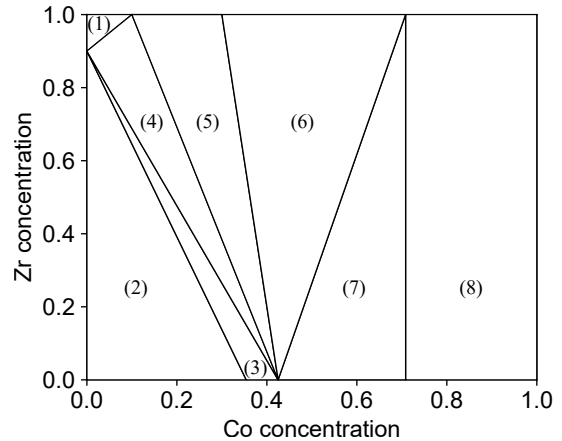


FIG. 3. Phase diagram on the  $(\text{Sm,Zr})(\text{Fe,Co})_{12}$  plane. (1)  $(\text{Sm,Zr})\text{Fe}_{12}$ ,  $\text{Zr}(\text{Fe,Co})_{12}$ ,  $\text{Zr}_2\text{Fe}_{17}$ , and unary Fe; (2)  $(\text{Sm,Zr})\text{Fe}_{12}$ ,  $\text{Sm}_2(\text{Fe,Co})_{17}$ , and unary Sm and Fe; (3)  $(\text{Sm,Zr})\text{Fe}_{12}$ ,  $\text{Sm}_2(\text{Fe,Co})_{17}$ , and unary Fe; (4)  $(\text{Sm,Zr})\text{Fe}_{12}$ ,  $\text{Zr}(\text{Fe,Co})_{12}$ ,  $\text{Sm}_2(\text{Fe,Co})_{17}$ , and unary Fe; (5)  $\text{Zr}(\text{Fe,Co})_{12}$ ,  $\text{Sm}_2(\text{Fe,Co})_{17}$ , and unary Fe; (6)  $\text{Zr}(\text{Fe,Co})_{12}$ ,  $\text{Sm}_2(\text{Fe,Co})_{17}$ ,  $\text{Zr}_2\text{Co}_{17}$ , and unary Fe; (7)  $\text{Sm}_2(\text{Fe,Co})_{17}$ ,  $\text{Zr}_2\text{Co}_{17}$ , and unary Fe; (8)  $\text{Sm}_2\text{Co}_{17}$ ,  $\text{Zr}_2\text{Co}_{17}$ , and unary Fe and Co.

$\text{ThMn}_{12}$  phases with  $\gamma = 0$  and 1, and the unary Ti phase. However, this does not preclude the existence of a metastable phase with  $\gamma = 0.5$ .

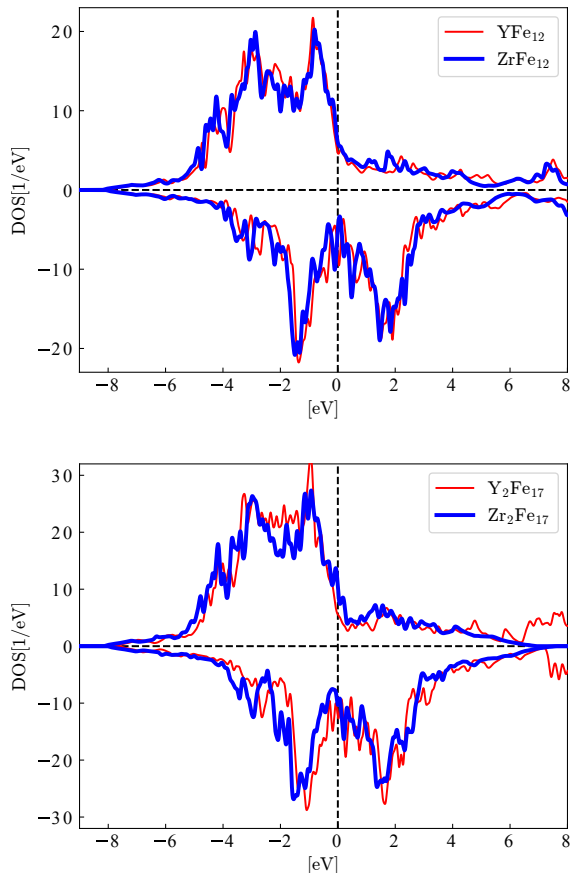


FIG. 4. Total DOS of (top)  $\text{YFe}_{12}$  and  $\text{ZrFe}_{12}$  and (bottom)  $\text{Y}_2\text{Fe}_{17}$  and  $\text{Zr}_2\text{Fe}_{17}$ .

### B. Hull distance

In this section, we examine the hull distance of  $(R_{1-\alpha}\text{Zr}_\alpha)(\text{Fe}_{1-\beta}\text{Co}_\beta)_{12-\gamma}\text{Ti}_\gamma$ , which is the energy difference from the stable separate phases. We compare these results with experimental reports, and roughly estimate the magnitude of deviation of the theory in a manner similar to how Ishikawa et al. estimated this for stoichiometric systems [48, 49].

Figures 5, 6, and 7 show the hull distance of  $(R_{1-\alpha}\text{Zr}_\alpha)(\text{Fe}_{1-\beta}\text{Co}_\beta)_{12-\gamma}\text{Ti}_\gamma$  for the  $R = \text{Y}, \text{Nd}$ , and  $\text{Sm}$  cases, respectively. In each of the figures, the top panel shows results with  $\gamma = 0$  (no Ti), the middle with  $\gamma = 0.5$ , and the bottom with  $\gamma = 1$ . Introducing Ti tends to decrease the hull distances of the  $\text{ThMn}_{12}$  systems and the Co-rich and Zr-lean region.

Although the formation of  $\text{ThMn}_{12}$  phases with compositions of  $(\text{Nd}_{0.7}\text{Zr}_{0.3})(\text{Fe}_{0.75}\text{Co}_{0.25})_{11.5}\text{Ti}_{0.5}$  and  $(\text{Sm}_{0.8}\text{Zr}_{0.2})(\text{Fe}_{0.75}\text{Co}_{0.25})_{11.5}\text{Ti}_{0.5}$  by the arc-melt and strip-cast method have been reported [21, 23, 24], these compositions are in the peak of the calculated hull-distance function, which suggests that those systems are energetically unfavorable. Phase separation into stabler

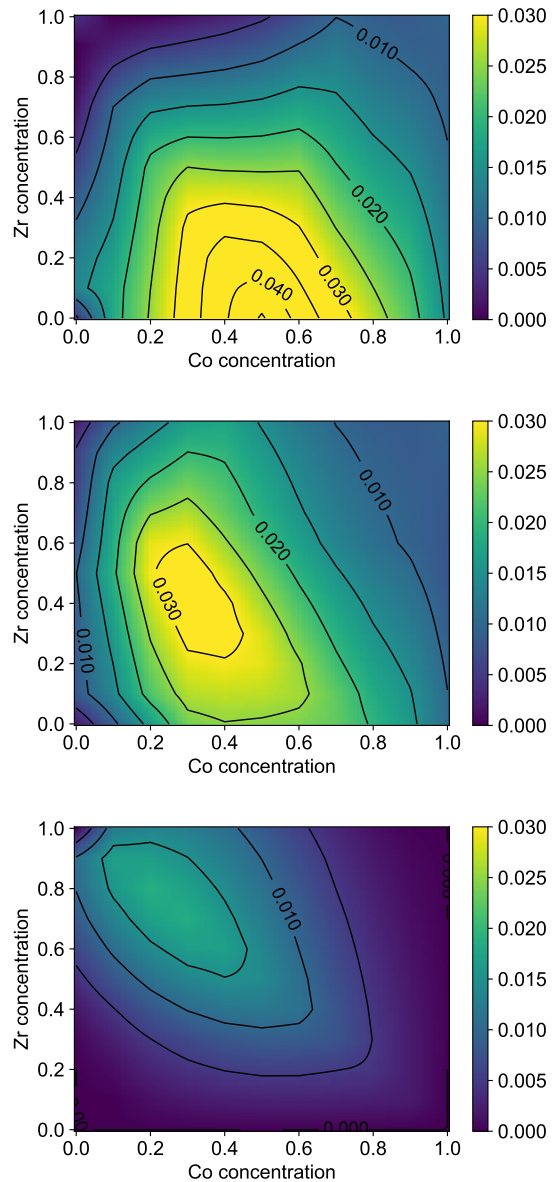


FIG. 5. Hull distance in eV for  $(\text{Y}_{1-\alpha}\text{Zr}_\alpha)(\text{Fe}_{1-\beta}\text{Co}_\beta)_{12-\gamma}\text{Ti}_\gamma$  with the  $\text{ThMn}_{12}$  structure with (top)  $\gamma = 0$ , (middle)  $\gamma = 0.5$ , and (bottom)  $\gamma = 1$ .

compositions may explain these results, and if this is the case, spatial inhomogeneity of elements is theoretically expected, which seems to be consistent with the microstructures observed experimentally by Suzuki et al. [21] and Kuno et al. [23].

Hirayama et al. have reported the epitaxial synthesis of films of  $\text{NdFe}_{12}$  [50, 51] and  $\text{Sm}(\text{Fe}_{1-\beta}\text{Co}_\beta)_{12}$  ( $\beta = 0, 0.1, 0.2$ ) [52], which had good homogeneity. The calculated hull distances of the films were in the range of  $\lesssim 30$  meV, and this value could be used as a criterion for possible metastable phases. Thus, we expect that it would be difficult to form a homogeneous system with a

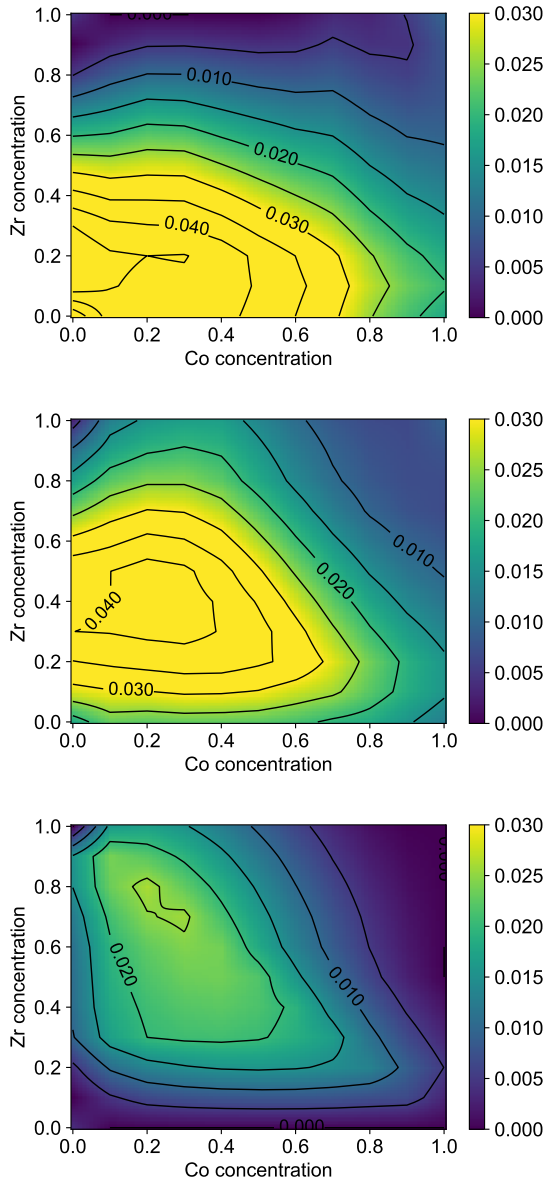


FIG. 6. Hull distance in eV for  $(\text{Nd}_{1-\alpha}\text{Zr}_{\alpha})(\text{Fe}_{1-\beta}\text{Co}_{\beta})_{12-\gamma}\text{Ti}_{\gamma}$  with the  $\text{ThMn}_{12}$  structure with (top)  $\gamma = 0$ , (middle)  $\gamma = 0.5$ , and (bottom)  $\gamma = 1$ .

Co concentration within  $0.3 \lesssim \beta \lesssim 0.7$ , although phases that are more Co-rich, such as  $R(\text{Fe}_{1-\beta}\text{Co}_{\beta})_{12}$  ( $\beta \gtrsim 0.7$ ), could be formed as a metastable phase.

#### IV. CONCLUSION

We examined the stability of  $(R,\text{Zr})(\text{Fe},\text{Co},\text{Ti})_{12}$  ( $R = \text{Y}, \text{Nd}, \text{Sm}$ ) with the  $\text{ThMn}_{12}$  structure based on first-principles calculations. We considered energetic competition among the unary phases, the  $(R,\text{Zr})(\text{Fe},\text{Co},\text{Ti})_{12}$  phases, and the  $R_2(\text{Fe},\text{Co})_{17}$  and  $\text{Zr}_2(\text{Fe},\text{Co})_{17}$  phases

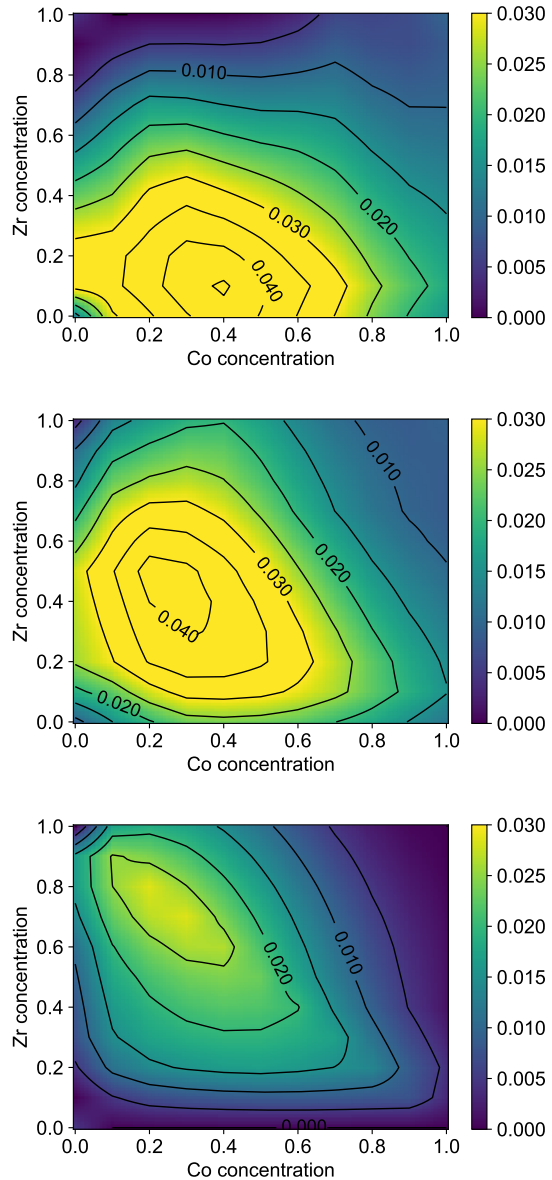


FIG. 7. Hull distance in eV for  $(\text{Sm}_{1-\alpha}\text{Zr}_{\alpha})(\text{Fe}_{1-\beta}\text{Co}_{\beta})_{12-\gamma}\text{Ti}_{\gamma}$  with the  $\text{ThMn}_{12}$  structure with (top)  $\gamma = 0$ , (middle)  $\gamma = 0.5$ , and (bottom)  $\gamma = 1$ .

with the  $\text{Th}_2\text{Zn}_{17}$  structure.

The  $\text{ThMn}_{12}$  structure was stabilized when the system was more Zr-rich and Co-lean. Zr stabilized the  $\text{ThMn}_{12}$  structure in the framework of the present calculation when the  $R$  site was mostly substituted by Zr. Although it has been reported that Co can stabilize the  $\text{ThMn}_{12}$  structure against the unary phases [26], we found that doping  $R\text{Fe}_{12}$  alone with Co did not lead to a stable phase of the  $\text{ThMn}_{12}$  structure because it stabilized the  $\text{Th}_2\text{Zn}_{17}$  phase.

We calculated the hull distance of  $(R,\text{Zr})(\text{Fe},\text{Co},\text{Ti})_{12}$  ( $R = \text{Y}, \text{Nd}, \text{Sm}$ ), and discussed the stability of exper-

imentally observed phases. The uniform distribution of Zr appeared to be energetically unfavorable from a theoretical perspective. By comparing our results with an experimental report for  $\text{Sm}(\text{Fe}_{1-\beta}\text{Co}_\beta)_{12}$  ( $\beta = 0, 0.1, 0.2$ ), we identified a hull distance of 30 meV as a criterion for possible metastable states. Provided this criterion is valid, formation of  $\text{Sm}(\text{Fe}_{1-\beta}\text{Co}_\beta)_{12}$  within the range of  $\beta \gtrsim 0.7$  should be possible as a metastable state.

### ACKNOWLEDGMENT

This work was supported by a project (JPNP20019) commissioned by the New Energy and Industrial Technology Development Organization (NEDO), the Elements Strategy Initiative Center for Magnetic Materials (ESICMM, Grant Number JPMXP0112101004), and the ‘‘Program for Promoting Researches on the Supercomputer Fugaku’’ (DPMSD, Project ID: JPMXP1020200307) by MEXT. The calculations were conducted in part using the facilities of the Supercomputer Center at the Institute for Solid State Physics, Univer-

sity of Tokyo, the supercomputer of the Academic Center for Computing and Media Studies (ACCMS), Kyoto University, and the supercomputer Fugaku provided by the RIKEN Center for Computational Science through the HPCI System Research Project (Project ID: hp200125, hp210179).

### Appendix A: Phonon dispersion in $\text{ZrFe}_{12}$

Some authors reported that they found no imaginary mode in  $M\text{Fe}_{12}$  for  $M = \text{Dy}, \text{Y}, \text{Sm}, \text{Nd}, \text{Ce}$ . [53, 54] Although it is preferable to calculate such phonon dispersions for all the systems predicted stable in Tables I–III to check the stability, doped systems need much computational resource in calculation. We instead see  $\text{ZrFe}_{12}$ , which has a close composition to the stable Ti-less  $\text{ThMn}_{12}$  phases, and need only a small unit cell in calculation. Figure 8 shows calculated phonon dispersion for  $\text{ZrFe}_{12}$  using the QMAS[38] and ALAMODE[55] package. There found no imaginary mode in the dispersion.

- 
- [1] K. Ohashi, Y. Tawara, R. Osugi, J. Sakurai, and Y. Komura, *Journal of the Less Common Metals* **139**, L1 (1988).
  - [2] K. Ohashi, Y. Tawara, R. Osugi, and M. Shima, *J. Appl. Phys.* **64**, 5714 (1988).
  - [3] Y.-c. Yang, L.-s. Kong, S.-h. Sun, D.-m. Gu, and B.-p. Cheng, *Journal of applied physics* **63**, 3702 (1988).
  - [4] R. Verhoef, F. De Boer, Z. Zhi-dong, and K. Buschow, *Journal of Magnetism and Magnetic Materials* **75**, 319 (1988).
  - [5] D. De Mooij and K. Buschow, *Journal of the Less Common Metals* **136**, 207 (1988).
  - [6] K. Buschow, *Journal of applied physics* **63**, 3130 (1988).
  - [7] S. S. Jaswal, Y. G. Ren, and D. J. Sellmyer, *J. Appl. Phys.* **67**, 4564 (1990).
  - [8] R. Coehoorn, *Phys. Rev. B* **41**, 11790 (1990).
  - [9] K. Buschow, *Journal of magnetism and magnetic materials* **100**, 79 (1991).
  - [10] S. Sakurada, A. Tsutai, and M. Sahashi, *Journal of Alloys and Compounds* **187**, 67 (1992).
  - [11] A. Sakuma, *J. Phys. Soc. Jpn.* **61**, 4119 (1992).
  - [12] S. Asano, S. Ishida, and S. Fujii, *Physica B: Condensed Matter* **190**, 155 (1993).
  - [13] M. Akayama, H. Fujii, K. Yamamoto, and K. Tatami, *J. Magn. Magn. Mater.* **130**, 99 (1994).
  - [14] M. D. Kuz'min, M. Richter, and K. H. J. Buschow, *Solid State Commun.* **113**, 47 (1999).
  - [15] A. M. Gabay, A. Mart'ın-Cid, J. M. Barandiaran, D. Salazar, and G. C. Hadjipanayis, *AIP Advances* **6**, 056015 (2016), <https://doi.org/10.1063/1.4944066>.
  - [16] W. K'orner, G. Krugel, and C. Els'asser, *Scientific Reports* **6**, 24686 (2016).
  - [17] L. Ke and D. D. Johnson, *Phys. Rev. B* **94**, 024423 (2016).

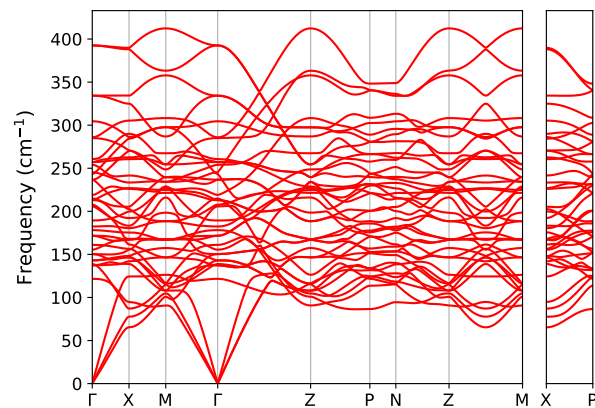


FIG. 8. Phonon dispersion for  $\text{ZrFe}_{12}$ .

- [18] T. Fukazawa, H. Akai, Y. Harashima, and T. Miyake, *Journal of Applied Physics* **122**, 053901 (2017).
- [19] T. Fukazawa, H. Akai, Y. Harashima, and T. Miyake, *Journal of Magnetism and Magnetic Materials* **469**, 296 (2019).
- [20] K. Ohashi, T. Yokoyama, R. Osugi, and Y. Tawara, *IEEE transactions on magnetics* **23**, 3101 (1987).
- [21] S. Suzuki, T. Kuno, K. Urushibata, K. Kobayashi, N. Sakuma, K. Washio, H. Kishimoto, A. Kato, and A. Manabe, *AIP Adv.* **4**, 117131 (2014).
- [22] N. Sakuma, S. Suzuki, T. Kuno, K. Urushibata, K. Kobayashi, M. Yano, A. Kato, and A. Manabe, *AIP Adv.* **6**, 056023 (2016).
- [23] T. Kuno, S. Suzuki, K. Urushibata, K. Kobayashi, N. Sakuma, M. Yano, A. Kato, and A. Manabe, *AIP Adv.* **6**, 025221 (2016).

- [24] S. Suzuki, T. Kuno, K. Urushibata, K. Kobayashi, N. Sakuma, K. Washio, M. Yano, A. Kato, and A. Manabe, *J. Magn. Magn. Mater.* **401**, 259 (2016).
- [25] H. Suzuki, *AIP Advances* **7**, 056208 (2017), <https://doi.org/10.1063/1.4973799>.
- [26] Y. Harashima, K. Terakura, H. Kino, S. Ishibashi, and T. Miyake, *Journal of Applied Physics* **120**, 203904 (2016).
- [27] Y. Harashima, T. Fukazawa, H. Kino, and T. Miyake, *Journal of Applied Physics* **124**, 163902 (2018).
- [28] T. Fukazawa, Y. Harashima, Z. Hou, and T. Miyake, *Physical Review Materials* **3**, 053807 (2019).
- [29] P. Hohenberg and W. Kohn, *Physical Review* **136**, B864 (1964).
- [30] W. Kohn and L. J. Sham, *Physical Review* **140**, A1133 (1965).
- [31] “AkaiKKR(Machikaneyama),” <http://kkk.phys.sci.osaka-u.ac.jp>.
- [32] J. Korringa, *Physica* **13**, 392 (1947).
- [33] W. Kohn and N. Rostoker, *Phys. Rev.* **94**, 1111 (1954).
- [34] J. Jensen and A. R. Mackintosh, *Rare earth magnetism* (Clarendon Oxford, 1991).
- [35] I. L. M. Locht, Y. O. Kvashnin, D. C. M. Rodrigues, M. Pereiro, A. Bergman, L. Bergqvist, A. I. Lichtenstein, M. I. Katsnelson, A. Delin, A. B. Klautau, B. Johansson, I. Di Marco, and O. Eriksson, *Phys. Rev. B* **94**, 085137 (2016).
- [36] M. Richter, *Journal of Physics D: Applied Physics* **31**, 1017 (1998).
- [37] J. P. Perdew and A. Zunger, *Phys. Rev. B* **23**, 5048 (1981).
- [38] “QMAS—Quantum Materials Simulator Official Site,” <http://qmas.jp>.
- [39] P. E. Blöchl, *Phys. Rev. B* **50**, 17953 (1994).
- [40] G. Kresse and D. Joubert, *Phys. Rev. B* **59**, 1758 (1999).
- [41] P. Soven, *Physical Review* **156**, 809 (1967).
- [42] P. Soven, *Physical Review B* **2**, 4715 (1970).
- [43] H. Shiba, *Progress of Theoretical Physics* **46**, 77 (1971).
- [44] “Qhull code for Convex Hull, Delaunay Triangulation, Voronoi Diagram, and Halfspace Intersection about a Point,” <http://www.qhull.org/>.
- [45] C. B. Barber, D. P. Dobkin, and H. Huhdanpaa, *ACM Transactions on Mathematical Software (TOMS)* **22**, 469 (1996).
- [46] T. Fukazawa, H. Akai, Y. Harashima, and T. Miyake, *IEEE Transaction on Magnetism* (in press).
- [47] J. Friedel and C. Sayers, *Journal de Physique* **38**, 697 (1977).
- [48] T. Ishikawa, T. Fukazawa, and T. Miyake, *Phys. Rev. Materials* **4**, 104408 (2020).
- [49] T. Ishikawa, T. Fukazawa, G. Xing, T. Tadano, and T. Miyake, *Phys. Rev. Materials* **5**, 054408 (2021).
- [50] Y. Hirayama, Y. Takahashi, S. Hirose, and K. Hono, *Scripta Materialia* **95**, 70 (2015).
- [51] Y. Hirayama, T. Miyake, and K. Hono, *JOM* **67**, 1344 (2015).
- [52] Y. Hirayama, Y. K. Takahashi, S. Hirose, and K. Hono, *Scripta Materialia* **138**, 62 (2017).
- [53] A. Saengdeejing and Y. Chen, *Journal of Phase Equilibria and Diffusion* **42**, 592 (2021).
- [54] G. Xing, T. Ishikawa, Y. Miura, T. Miyake, and T. Tadano, *Journal of Alloys and Compounds* **874**, 159754 (2021).
- [55] T. Tadano, Y. Gohda, and S. Tsuneyuki, *Journal of Physics: Condensed Matter* **26**, 225402 (2014).